Laser Micromachining

Udo Klotzbach, Andrés Fabián Lasagni, Michael Panzner and Volker Franke

Abstract Over the recent years, the laser technology and its potentials have been exciting laser manufacturers as well as researchers and industrial users. Lasers with their excellent beam quality promised noticeable advantages and improvements in high precision and material processing at the microscale. Besides the excellent beam quality there are more advantages of the laser technology such as compact installation size, high laser efficiency, moderate system price and easy to be integrated. This chapter describes the results of different short pulse laser systems in a wide field of applications, showing specific advantages in practical applications. Typical applications of laser micro machining have been chosen including drilling, cutting, structuring, lateral material removal as well as marking.

1 Introduction

The excellence attributes of laser radiation combined with a high degree off flexibility, contact- and wear-less machining, the possibility of high automation as well as easy integration allows using this tool in a wide field of macro machining processes for many materials including silicon, ceramics, metal and polymer.

The world of laser machining production is divided into micro- and macro-machining. This classification is not based on the size of the work piece but rather the fineness of the impact cased by the laser tool. The lasers system used for micromachining employ normally pulsed beams with an average power of well

U. Klotzbach (✉) · A. F. Lasagni · M. Panzner · V. Franke
Fraunhofer Institute for Material and Beam Technology (IWS),
Winterbergstr. 28, 01277 Dresden, Germany
e-mail: udo.klotzbach@iws.fraunhofer.de

F. A. Lasagni and A. F. Lasagni (eds.), *Fabrication and Characterization in the Micro-Nano Range,* Advanced Structured Materials, 10,
DOI: 10.1007/978-3-642-17782-8_2,

below 1 kW while those used for macro machining use generally continuous-wave (CW) laser beams ranging up to several kW.

Laser micromachining techniques are currently used by the automobile and medical industries as well as in the production of semiconductors and solar cell processing.

Lasers for micromachining offer a wide range of wavelengths, pulse duration (from femtosecond to microsecond) and repetition rates (from single pulse to Megahertz). These attributes allow micromachining with high resolution in depth and lateral dimensions.

The field of micro-machining includes manufacturing methods like drilling, cutting, welding as well as ablation and material surface texturing, whereby it is possible to achieve very fine surface structures ranging in the micrometer domain. Such processes require a rapid heating, melting and evaporation of the material. The use of extremely short nano- and pico- and even femtosecond pulse durations helps to minimize the thermal effects such as melting and burr formation thus eliminating the need for any post processing measures.

Besides choosing the proper laser source, it is often necessary to employ specialized micromachining components in order to achieve a desired geometry. Currently, laser micromachining is accomplished with two technologies: (i) direct laser writing (DLW) using solid state lasers with a 2D galvanometer scan head, and (ii) mask projection technique (MP) using mostly Excimer lasers and conventional fixed masks.

In DLW, hard or low-sensitive materials generally require solid state lasers in combination with galvanometer scan heads and focussing optics to minimize the beam diameter and guide it over the material surface (Fig. 1).

Based on today's approved scan head technologies and software, even processing of three dimensional surfaces is possible. Advantages are simple programmability and the resulting flexibility. Generation of characters, barcodes and other patterns is easy. Compatibility to existing file formats like "DXF" (Drawing Interchange Format) or "PLT" (Plot File) is given by the software's import features. In consequence, this process can be easily controlled, permitting a high flexibility.

Limitations of the direct writing process are given by the inherent characteristic of the sequential information transfer and dynamics of the scan head. In consequence there is speed limitation that must be considered. A second and often even more important limitation is given by the generally high intensities, which result from high power and tight focusing of the laser beam. Therefore marking of sensitive materials like paper or plastics is hard or even impossible.

For sensitive materials (especially organic materials) often Excimer lasers are used. Compared to frequency tripled solid state lasers their benefit is that even shorter wavelength can be utilized which allows to permanently change the color of UV-absorbing pigments like titanium oxide. These lasers are commonly used in mask projection techniques (MP). Like in photolithography, the mask projection technique enables to transfer all information contained in a fixed transmissive mask at once (Fig. 2). In addition to that, the laser beam must be collimated and

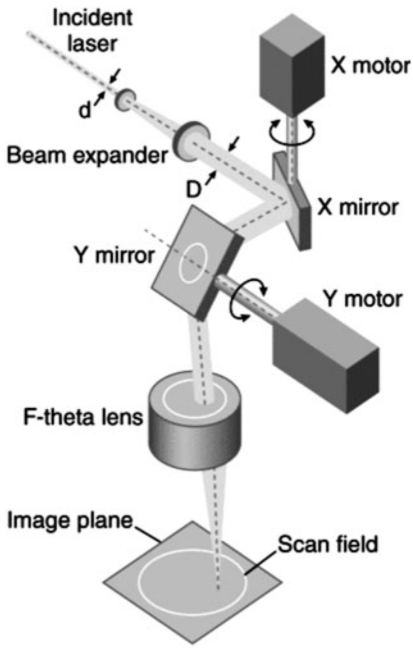

Fig. 1 Principle of direct laser writing method with *xy*-galvanometer scan-head

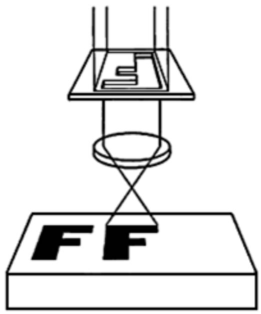

Fig. 2 Principle of mask projection technique

homogenized before illuminating the mask, and the projection system permit to control the size of the projected two dimensional objects.

With this technique a complete marking of alphanumeric characters or pictures is generated within one laser pulse which typically has a length of some nanoseconds. In this way, the process speed is just limited by the repetition rate of the Excimer laser and not by mechanical movement of mirrors with galvanometer scanners. However there is evidently a drawback of the technique, since each new marking requires a new mask.

2 Laser Micro Structuring of Silicon

Micro structures in silicon are applied in different industrial fields as well as in medicine and research. Examples are micro mechanical sensors for car security systems, nozzle plates for printer, and optical elements for X-ray beam splitting. Wherever the accuracy of etched silicon structures is not required, laser processes with short pulses and small wave length can be an option with the advantage of shorter process time.

High quality cutting and drilling of silicon can be achieved by application of diode pumped q-switched Nd:YAG-lasers and harmonics generation. The short pulses (<15 ns) and the UV wavelength (e.g. 266 and 355 nm) for example, allow a reduction of thermal effects like deposition of molten material and heat effected zones (HAZ) at the edges. Especially, in the case of deep structures, the ablation plasma causes strong heating of the walls. A reduction of the plasma temperatures and so the heat influence on the walls can be realized by using smaller laser wavelengths with low plasma absorption. Short laser pulse durations are necessary to reduce the heat affected depth or melting due to heat flow from the ablation area into the bulk material. Also the duration and intensity of plasma heating is reduced by short laser pulses.

In this section the possibilities and limits of laser machining of silicon by diode pumped Nd:YAG-lasers with harmonics generation are discussed.

2.1 Interaction of Laser Radiation with Silicon

Silicon is one of the most thoroughly investigated materials. The vast majority of electronic components are based on semi-conducting mono-crystalline silicon. Polycrystalline and amorphous silicon is used in solar cell technology. Micro-mechanical components as acceleration sensors in car safety systems and micro-fluidic circuits are made of silicon. Silicon is also used as a substrate for X-ray mirrors.

Each of the above mentioned applications involves the structuring of the bulk material since this material cannot be directly processed as pre-formed parts, with the necessary quality requirements. In general, the high accuracy necessary for micro-mechanical components with their structural dimensions of typically a few micrometers is realized with etching technology. Mechanical cutting with its lower accuracy is applied for separating the chips on the wafer. Also laser induced etching [1] is coming up as new emerging process technology. Laser processing has an accuracy intermediate between etching and mechanical cutting, combined with the essential advantage of high flexibility: the beam spot on the material can be rapidly moved by scanning, and/or the sample can be moved below the spot.

The technology applied for a special purpose is chosen according to several quality criteria including:

(i) amount of deposited material along the edges,
(ii) width of damaged material along the edges,
(iii) minimum structural dimensions,
(iv) maximum flank slope, smoothness of flanks and bottom.

The accuracy of structuring with pulse laser depends on wavelength, pulse time, pulse repetition rate, and intensity distribution on the beam spot, as well as on the beam guiding technique.

Much effort has been done in application of short pulse laser technology for silicon processing [2, 3]. When comparing femtosecond laser technology and ns-laser technology, it appears that industrial requirements can be more easily satisfied with ns-lasers.

Improved accuracy of silicon structuring can be expected from using harmonics with their shorter wavelength instead of the original IR-beam of the Nd:YAG-laser. The penetration depth of the beam into the material is usually quantified by a decay length, here denoted as x_{opt}, which is the inverse of the absorption coefficient $\alpha(\lambda)$. Note that its dependence on the wavelength λ may be very strong as seen in Fig. 3. In case of very small penetration depths, there is a high concentration of deposited power per pulse so that essentially the whole heated layer can be removed while the amount of melt can be negligibly small. In case of larger penetration depths and correspondingly lower concentration of deposited power per pulse, a larger amount of melt is present but the rate of removal may be low.

The decay lengths (or optical penetration depth) of the Nd:YAG-laser radiation and its harmonics as derived from Fig. 3 are 60, 0.5 and 0.01 μm for wavelengths of 1064, 532, and 355 nm, respectively.

Whether the optical penetration depth is a relevant quantity here depends on the comparison with the thermal penetration depth x_{th} related to the thermal diffusivity κ of the material

$$x_{th} = (\kappa\tau)^{1/2}, \quad \kappa = \frac{\lambda}{\rho c} \tag{1}$$

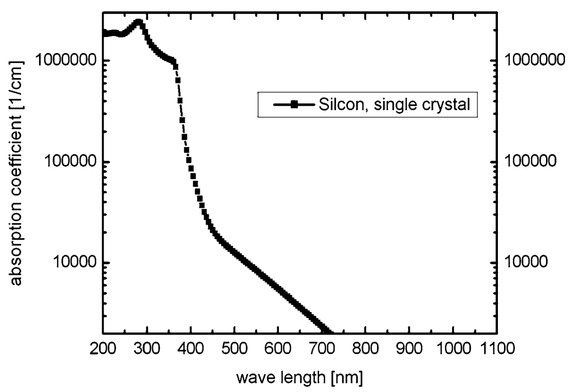

Fig. 3 Absorption coefficient in dependence on wave length [6]

where ρ is the density, c is the specific heat, and τ is the pulse duration

Obviously, shorter pulses lead to smaller thermal penetration depths. For 15 ns pulses, the thermal penetration depth is $\sim$4 μm in silicon.

Apart from that, the accuracy of the generated structure and the quality of its edges are influenced by the ablation plasma. Especially within deep holes, plasma can lead to melt formation at the wall and to removal of material in places where it is not to be removed [4].

To avoid exceedingly high plasma temperature, the absorption by inverse Bremsstrahlung should be kept low. As the plasma absorption α_p goes with the inverse square of the frequency [5],

$$\alpha_p \approx \frac{n}{\nu^2} \cdot e^{(\Delta E_0)/kT_e} \tag{2}$$

where n is the electron density, k is the Boltzmann constant, T_e is the electron temperature, ΔE_0 is the energy gap, and ν is the light frequency.

Higher frequencies or shorter wavelengths produce a lower absorption and hence lower temperatures.

Melt formation may also cause problems as the melt driven out of the hole by the plasma pressure can get stuck to the cooler parts of the borehole wall. From the above considerations it can be deduced that diode-pumped solid-state lasers with harmonics generation and pulses $\tau < 30$ ns, which have become commercially available only recently, should be suitable for high-accuracy structuring processes on silicon.

Next, several examples of micro-processing possibilities using laser radiation on silicon are described. The experiments have been done with a frequency-doubled Nd:YAG-laser and a frequency-tripled Nd:YAG-laser with average powers of 13.5 and 3 W, respectively and a repetition rate of 10 kHz for both cases.

2.2 *Single Pulses and Percussion Holes*

The focused laser beam spot was moved over the silicon surface by means of scanner with a path velocity as high as 6.5 m/s so that with 10 kHz repetition rate the effect of the individual pulses was resolved, as seen in the SEM images (Fig. 4). A 15 μm wide crater was formed, surrounded by a 40 μm wide area covered with splashed melt.

With stationary spot, through holes are formed after 20,000 pulses (Fig. 5). In this case, the beam was focused on the surface of the sample, producing a hole with 25 μm in diameter at the entry and 20 μm at the exit. Then, the taper ratio (T) for this case was $\sim$0.9% calculated using Eq. 3. The last parameter can be related with the quality of the produced hole:

$$T\% = \frac{d_{\text{entry}} - d_{\text{exit}}}{\text{th}} \cdot 100\% \tag{3}$$

where th is the substrate thickness

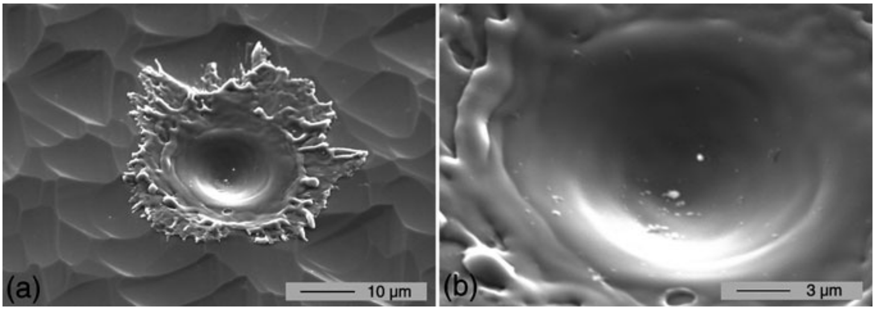

Fig. 4 SEM-images of the effect of single UV pulses on an unpolished Si (111). **a** Surface overview of the whole spot and **b** its internal region with a higher magnification (sample is slightly tilted for better visualisation)

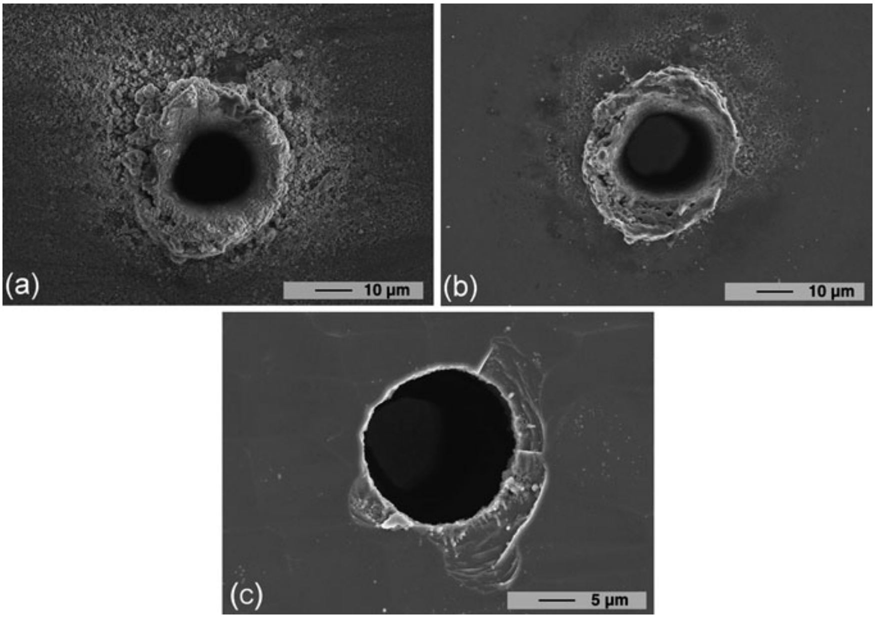

Fig. 5 SEM images of percussion holes in Si (111), thickness 550 µm, 20,000 pulses, 10 kHz: **a** hole entry without HF-cleaning, **b** hole entry after HF-cleaning, **c** hole exit

After structuring, the substrates were etched with 20% hydrofluoric acid and rinsed with distilled water to remove deposits of Silicon oxide along the edges. The effect of hydrogen fluoride (HF) cleaning is distinctly visible: the deposited Silicon oxide is removed. However, the cleaned surface seems to be slightly rough. A molten rim may be also formed around the entry edge of the hole.

2.3 Silicon Cutting

With the short wavelengths and short pulses applied here, the laser beam erosion of Silicon is dominated by sublimation. However, it is obvious that transient melting is also part of the process.

The depth of trenches obtained with repeated erosion cycles is plotted in Figs. 6 and 7 for two beam-path velocities for both wavelengths. The erosion rate has always been found larger at the beginning and becoming nearly stationary, with some fluctuations, at a depth of about 200 µm. In the case of cutting thick samples we found erosion stopping because of enhanced beam reflections at the trench walls for smaller spots. Wider trenches allow deeper cuts.

The cause for this trend is not obvious. As expected from Fig. 3, the erosion rate at 355 nm should be higher than at 532 nm. Because of the low accuracy of depth measurement, the difference in the erosion rate for 5 and 100 mm/s path velocities seems to be insignificant. The cross-shaped cut in a 550 µm silicon wafer (see Fig. 8a) gives an impression of the cut quality, which is even higher for thinner substrates since less heat accumulation and melting near the edges are produced during the cutting process (Fig. 8b). Cutting with 335 nm beam produces smaller amounts of melt and hence higher quality. The obtained gap widths are 40 and 100 µm, respectively.

Figure 8b shows a section through a 550 µm wafer cut with UV-laser (355 nm). The taper angle of the gap is 88.3° and the width is 18 µm below (Fig. 9a), with higher edge quality than above.

In addition to straight cuts or simple geometries, by combining the correct solid-state laser with a flexible and well controllable scanner, structures suitable for micro-mechanics and micro-fluidics can be also easily produced. For demonstration, a toothed gear has been cut from a 550 µm silicon slab (Fig. 9b). The clean edges have been obtained with hydrofluoric acid etching as described above.

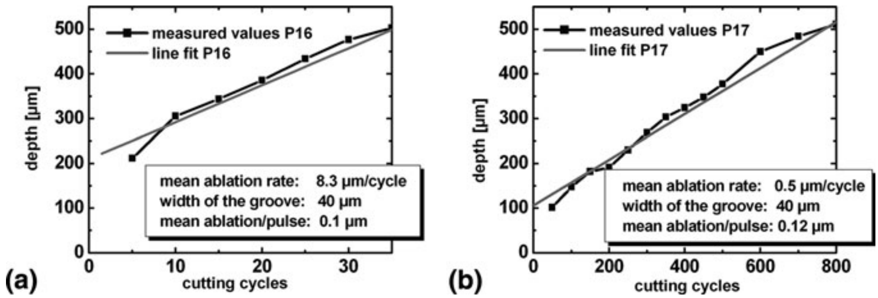

Fig. 6 Cutting depth in dependence on the number of cutting cycles. Sample Si (111), thickness ~550 µm: **a** UV-laser, cutting velocity 5 mm/s; **b** UV-laser, cutting velocity 100 mm/s

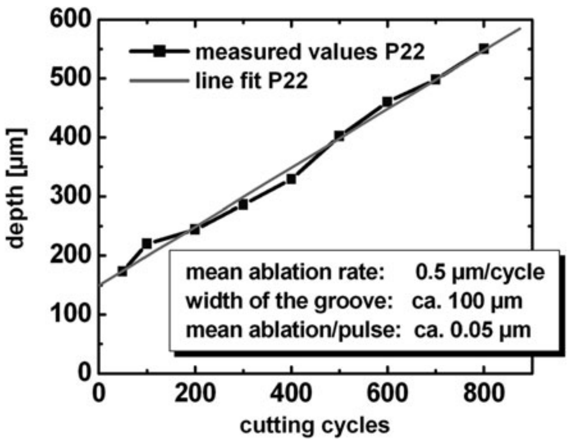

Fig. 7 Cutting depth in dependence on the number of cutting cycles. Sample Si (111), thickness ~550 µm. 532 nm laser, cutting velocity 100 mm/s

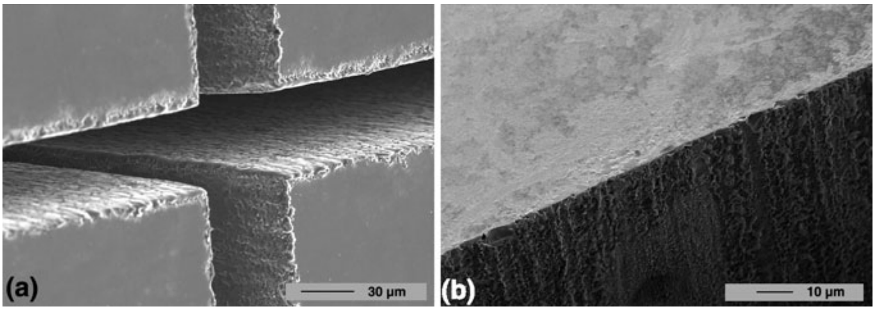

Fig. 8 Silicon wafers cut at 355 nm: **a** crossed cuts in 550 µm wafer (beam entry) and **b** cut in 355 µm wafer (beam entry)

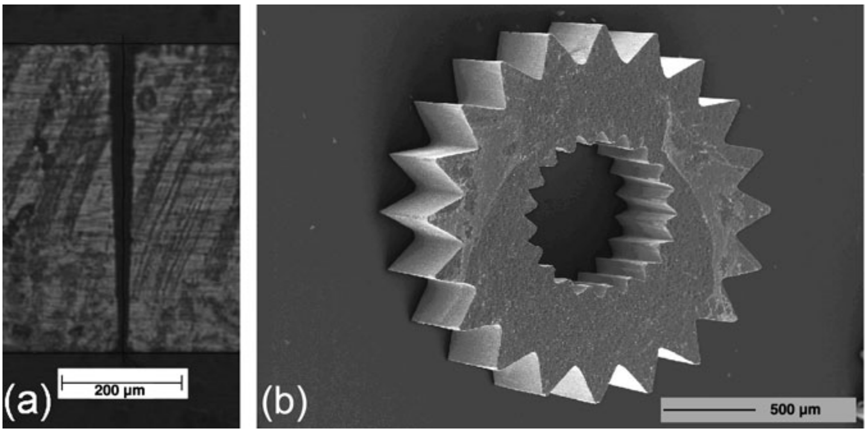

Fig. 9 **a** Silicon wafers cut at 355 nm, section of cut on 550 µm wafer; **b** toothed gear cut with UV-laser

2.4 Mask Projection Ablation of Silicon

2.5-D structures in silicon as applied in micro-fluidics devices, for example, are usually produced by means of a mask projection technique with a homogenized Excimer radiation [7]. The alternative technique by scanning a frequency tripled Nd: YAG-laser beam produces rougher faces because of the localized irradiation. In order to apply this flexible technique nevertheless, quantitative information on the resulting roughness has to be obtained, and ways to minimize this roughness have to be found.

A process parameter that could affect both the ablation depth as well as surface roughness of the final treated area is the number of scans realized, between others. This effect is depicted in Fig. 10. The rectangular pit in Fig. 11 has been obtained by line-wise scanning, with the line direction switched by 40° after every coverage of the area, with nine area scans. The bottom face obtained in this way is fairly well isotropic compared to faces obtained with conventional scanning in two directions. As expected the erosion rate varies essentially inversely with the scanning velocity (Fig. 10). The micro roughness of about 0.8 µm on average is found to be nearly independent of velocity and number of scans but dependent on line spacing. In these investigations, the optimum spacing of 10 µm was chosen.

2.5 Summary

The presented results demonstrate that frequency doubled or tripled solid-state lasers with ultraviolet or green wavelength are suitable for structuring silicon. By judging the obtained accuracy and erosion rate in relation to the effort, the 355 nm is more favourable than the 532 nm wavelength. Although laser structuring does not reach the accuracy of etching, its flexibility and high rate make it a promising

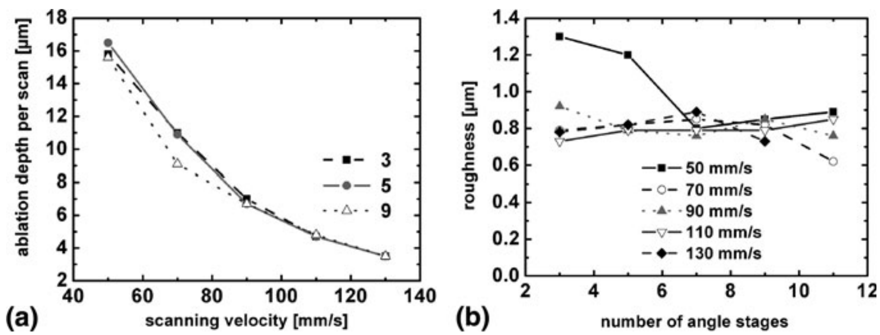

Fig. 10 Processing scanning parameters with changing direction. **a** Average ablation depth per single scan for several numbers of scans; **b** surface roughness for several velocities and numbers of scans

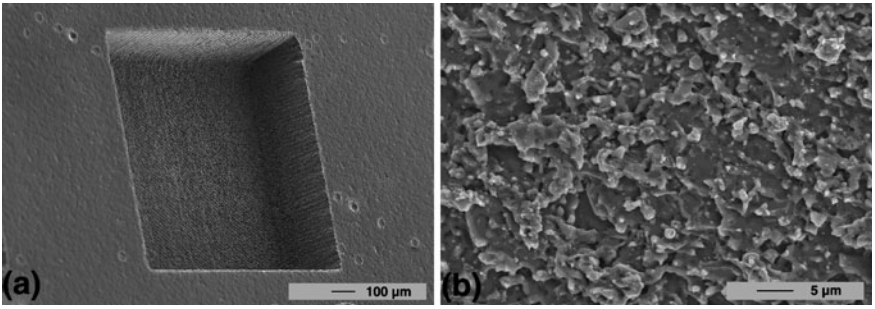

Fig. 11 Erosion of Si (111) face with UV radiation (335 nm): Beam power on sample: 1.1 W, nine scans differing by 40° line direction; scan velocity 70 mm/s. **a** Survey and **b** bottom face magnified

technique, especially in a parameter range where mechanical tooling meets its limits. This technique is expected to be suitable for producing structures in micro-mechanics, micro-fluidics, and processing of materials for sensors/semiconductor and photovoltaic [8]. In particular, the cutting of irregular-shaped sensor chips might be a promising application.

3 Laser Joining of Low Temperature Cofired Ceramics and Polymers

Low Temperature Cofired Ceramics (LTCC) represent a key technology for the realization of electronic high-frequency systems due to their possible integration into design three-dimensional circuits. Generally, electrical components are produced by screen process. The prepared LTTC foils are stacked, pressed and sintered at high temperature (e.g. 900°C), and utilizing the so called multilayer technology. Three-dimensional ceramic micro structures (like chambers, cavities, channels, through holes) and highly integrated electronic circuits such conductor paths, sensors (e.g. pressure sensor, pH measurement, conductivity, impedance), and actuators (e.g. piezoelectric oscillator) can be realized.

Apart from that, it is also feasible to manufacture large micro-fluidic systems on basis of LTCC ceramic. Those systems are more expensive than equal systems made of polymer due to higher material and processing costs. This technology allows a high flexibility in rapid prototyping of micro reactors and for example online controlling for cell growing with optical microscopy. Compared to a classical stainless steel micro reactor it is possible to integrate electrical sensors or actors—like a impedance measurement system. Another disadvantage of ceramic systems is that the material is not transparent and therefore not suitable for optical analyses. This requirement is necessary to monitor different processes simultaneously as in different areas of biological and medical investigation fields.

To solve this problem, transparent windows (e.g. made of polymer) need to be integrated into the ceramic sensor system.

Different technologies for joining of polymers and ceramic parts are known and established in industrial manufacturing processes. For example, the polymer and ceramic parts can be glued using different kinds of adhesives such organic or inorganic adhesives. The additional material (adhesive) is linking to both joining partners in a chemical (dissolving and mixing) or mechanical (anchoring) way. Another method consists on using mechanical joining techniques like screws or clamps. However, additional features like through holes or notches need to be integrated into the polymer and ceramic sub-assemblies. Using those mechanical joining methods it is difficult to realize gas-proof hermetic joints between the joining partners without inserting an additional sealing.

Laser joining methods have also been employed to join ceramic substrates to other materials (e.g. metallic contacts) [9]. In the last case laser radiation is transmitting through the ceramic joining partner toward the metal joining partner and thus heating both parts as well as the solder. Another common laser joining technique is laser welding of polymers. In this case, both joining partners, made of similar thermoplastic polymers, are irradiated through the first, partly transparent part, while the second part is absorbing the laser radiation. Due to heat conduction processes, the adjacent transparent part is also heated up and thus the material within the contact area is melting and mixing up. After solidification process, the joint has the same properties as the base material.

In the case of ceramic-polymer joining, the materials to be joint have extremely different thermal and physical characteristics. The melting ($\sim$ 100–300°C) and pyrolysis temperatures of common thermoplastic polymers are well below the melting temperatures of common ceramics ($\sim$ 1,000°C). The pyrolysis (thermal destruction) of most common polymers starts below 400°C. Therefore it is impossible to melt and mix both materials for joining purposes. Hence the basic idea of the novel joining technique is to melt the polymer part and pressing the molten material into the roughness and pores of the solid ceramic part. In this way no chemical or material joint is realized but a combination of adhesion and mechanical anchoring between both joining partners.

3.1 The Joining Process

Two different laser sources have been used in recent studies: (i) a standard Nd:YAG solid state laser (Rofin Sinar system RS Marker 100D) and a novel fiber laser system (Ytterbium fiber laser 100C-13-R06), manufactured by SPI. Both systems are emitting continues wave (cw) and pulsed radiation within the near infrared spectrum (1,064 and 1,090 nm, respectively). In addition, different focusing optics with focal lengths between 50 and 300 mm have been used for the joining tests. To realize the relative motion between beam and the joining partners two different systems were utilized. A fixed focusing optic can be combined with a

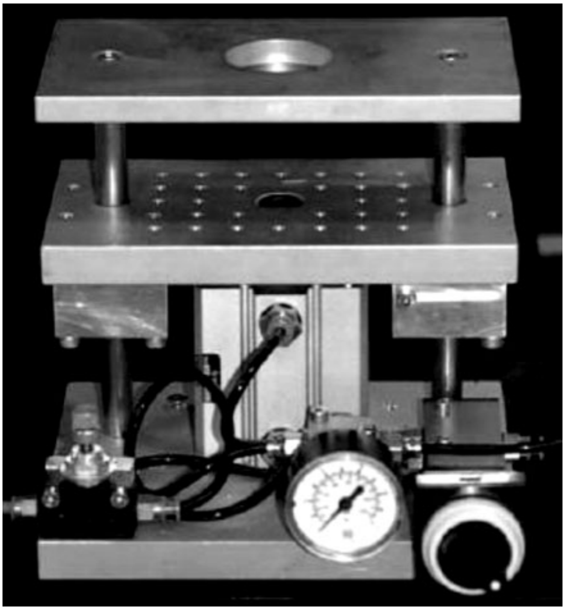

Fig. 12 Pneumatic clamping fixture utilized in the laser joining process

three-axis motion system. The second option is to use a galvanometer scanner for beam deflection. Two pivotable mirrors inside are deflecting and moving the laser beam within a limited marking field. In this case no relative motion of optics and joining parts is needed.

A relevant part of the equipment is the pneumatic clamping fixture depicted in Fig. 12. The joining partners are positioned on top of each other and placed between the upper two plates of the clamp. A cut-out of the upper plate allows the laser beam to reach the joining area. Both parts are pressed against each other with an adjustable pressure.

The clamping fixture has two main functions: realizing a close contact and creating pressure within the molten polymer. A close contact between polymer and ceramic is needed to ensure effective heat conduction between both parts. In addition, it is required that the laser radiation passing through the transparent polymer is not absorbed. When reaching the ceramic part, the radiation is absorbed and converted into heat. Therefore, the heat is conducted from the ceramic to the polymer (the smaller the gap the better the heat transition).

Before joining both materials, the surfaces must be treated. The surface of the ceramic has to be rough or porous enough to ensure that a sufficient density of anchoring points is available for the polymer. The used LTCC parts used for the study show a relative low surface roughness ($R_a \sim 0.5$ µm). In this state the surface is too smooth to realize a strong and reliable bond. In a first step, the LTCC surface was roughened using sandpaper realizing a surface roughness of $R_a = 3.8$ µm ($R_z = 19$ µm). First successful joints were realized using these mechanically treated surfaces. For more extensive studies, the structuring process

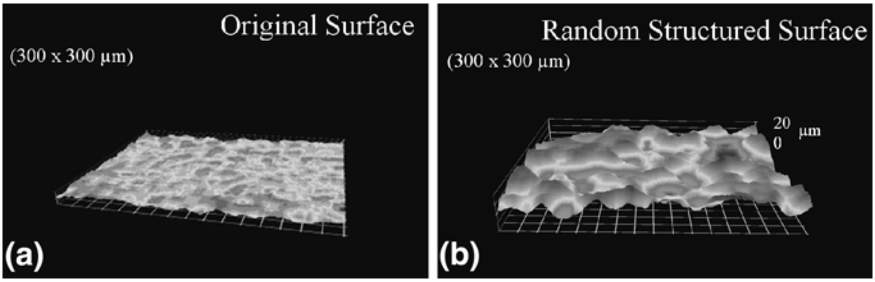

Fig. 13 **a** Unstructured (original) and **b** structured surface with random shot

Table 1 Varied parameters of linear- and dot-shaped structure

Laser pulse frequency (kHz)	Line distance (mm)	Average output power (W)	Structuring velocity (mm/s)
5; 10	0.05; 0.2; 0.7; 1	2; 7; 12;	200; 400; 800; 1,000; 1,500
Laser pulse frequency (kHz)	**Dot density (mm^{-2})**	**Average output power (W)**	**Structuring time per dot (ms)**
10	8.5; 17; 34; 68	15; 20	0.7; 1.0

was accomplished utilizing laser material ablation techniques with pulsed laser radiation [10, 11]. User-defined surface structures (dot- and line-shaped) with different geometrical parameters (such line-distance, density of dots per unit of area, etc.) were fabricated. The programmable laser structuring process offers a high flexibility of the geometries that are generated. Figure 13 shows an example of a typical LTCC surface before and after laser micro structuring. In this case, the Rofin Sinar RS Marker 100 D was used in pulsed "Q-switch mode" with a fixed laser spot size of approximately 100 µm. Therefore the lateral sizes of the single structures (dot- or linear-shaped) were limited to these dimensions (crater diameter or line width). The laser parameters to produce the structures are listed in Table 1.

After preparation of the ceramic surface, the joining partners are placed inside the pneumatic clamping fixture with the polymer part on top, and external pressure is applied. Then, the parts are scanned using the laser radiation (Fig. 14a). If the temperature within the joining area exceeds the fusion temperature of the polymer, a thin layer of molten, high-viscosity polymer is generated. The external pressure is forcing the macromolecules to move into the cavities of the solid ceramic surface (Fig. 14b). When the laser beam has passed or is switched off, the joining area is cooling down due to heat conduction into the bulk material, and the molten polymer solidifies. After the complete part is joined and cooled down the pneumatic clamping fixture can be released. The mechanical anchoring between polymer and the ceramic persists and both parts are joined.

Different laser and process parameters are influencing the property of the joint, e.g. laser output power, joining velocity, intensity, beam diameter, joining pressure

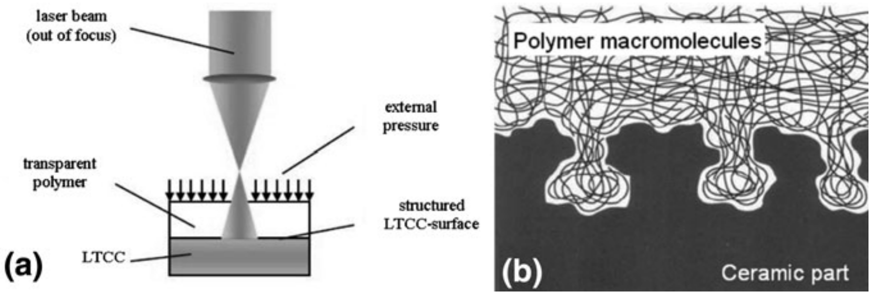

Fig. 14 **a** Principle of the joining process. **b** Schematic of the joined contact area

and surface structure of the LTCC part. For a specific application and material combination the process parameters need to be adjusted. Experimental results showed only minor influence of the external pressure on the joints mechanical strength. The beam intensity is a function of the laser power and the beam diameter. It is defined as the quotient of power and cross-sectional area of the beam. The beam diameter at the joining area can be changed by applying different optics or by changing the focus position (defocusing). By changing the beam diameter (and laser output power) the resulting line width of the joint can be influenced. The beam diameter in focus position approximately defines the minimum line width possible. Several of these parameters are linked to each other, e.g. laser output power, joining velocity and line width. The energy input per unit length is defined as the quotient of power and velocity. Thus the energy input per unit length can be increased by increasing the output power and by decreasing the velocity. This quotient divided by the line width gives the energy input per unit area.

Depending on the energy input per area unit different joining results are emerging. Figure 15 illustrates the changes in the appearance when the energy input is increased. The tensile strength of the joint is influenced as well. In general the tensile strength is rising when increasing the energy input until a maximum strength is reached. When the energy input is too low no joint is generated. Example i shows first reactions of the polymer within the irradiated area. But the amount of molten polymer is too small to flow into the cavities of the ceramic surface. When increasing the energy input (examples ii and iii) the temperature and the amount of molten material increases. The higher temperature reduces the viscosity of the molten material and therefore avails the ability to flow into the ceramic surface. Example iii shows a homogeneous joint without gaps or bubbles. Tensile strength reaches its maximum. Further increasing of the energy input leads to overheating of the molten polymer material (examples iv and v). Small bubbles, a channel in the center and cracks appear within the joint. The tensile strength is decreasing. If the energy input is increased even more, the temperature exceeds the pyrolysis temperature of the polymer resulting in strong thermal damages (example vi).

Concerning to the effect of surface topography of the LTCC parts, the following results were observed. For the smooth untreated LTCC surface, although it was possible to melt the polymer at the joining surface, no strong anchoring between

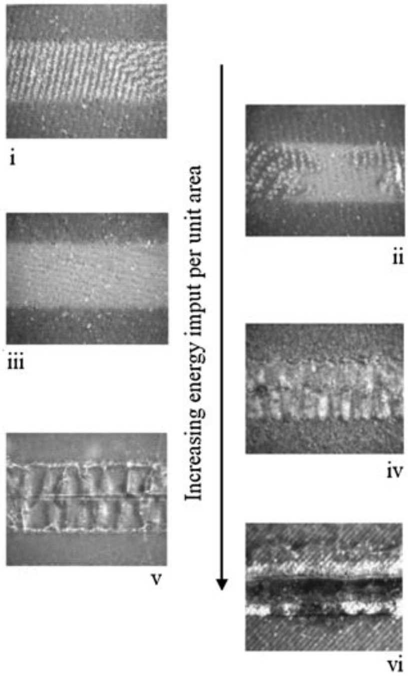

Fig. 15 Different joints depending on energy input (Top-view). The polymer is transparent

both parts was observed. A roughness of $R_a = 0.5$ μm provides an insufficient number and size of anchoring points like cavities to ensure a strong bond. After that, the tensile strength of joined assemblies was tested for a variety of the different patterns and combinations of both patterns. The studies also showed that both structuring patterns are suitable to achieve mechanically strong, reliable and hermetic joints. Both structuring systems reached tensile strengths with similar values. Moreover, recent studies demonstrated that joined parts with a combination of linear and dot-shaped structures achieved the highest tensile strengths (19 N/mm^2). In general, it was observed that the tensile strength is rising when depth and size of the laser generated structures are increasing up to a certain point. When the surface gets too rough, the joint is becoming weaker again. In the last case, more polymer material needs to be molten and pressed into the roughness. But the rough surface decreases heat conduction into the polymer part and therefore hampers the joining process. Thus a compromise has to be found.

3.2 LTCC Based Sensor Example

A LTCC multilayer system consisting of five layers as depicted in Fig. 16 was designed and built. Each layer includes four identical subassemblies of the lab-on-a-chip system. In addition, large circular apertures building up the cell

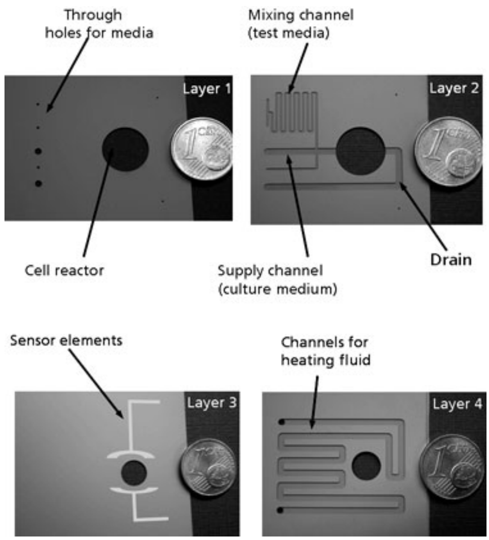

Fig. 16 LTCC multilayer with microfluidic components and impedance sensors

reactors when stacked up were included. At the bottom of layer 4, a large meander like channel is implemented, which is flushed with a tempered fluid to hold a constant temperature within the cell reactor. Above, on layer 3, LTCC based sensors are integrated to measure both impedance and temperature. By drilling different holes, electrical connection within the layers was performed. Impedance measurements are used to monitor changes in cellular growth, e.g. adsorption of cells on a surface. In addition, different media can be fed through the micro channels in layer 2.

This meandrous structure gives the opportunity to mix two different testing liquids or dilution. The through holes of the upper and bottom layers (layers 1 and 5) are used to connect the lab-on-a-chip system to the required supply units and electronic measurement equipment [12].

3.3 Summary

A novel technique permitting the opportunity to join two extremely different materials (polymer and ceramic) without any additional glue or mechanical devices was developed. The joining process is divided into two steps: (i) surface preparation of the ceramic and (ii) laser based partial melting of the polymer part. The joining results are particularly influenced by the energy input per unit area and the shape of the laser structured ceramic surface. Hermetic joints and tensile strength of 19 N/mm^2 were achieved. Based on the technology a lab-on-a-chip system was developed as a first application.

The basic technological principle of the joining technique can also be transferred to join polymers with semiconductors or metals for instance. Promising applications and request for the joining technology are expected in the field of biological and chemical analysis.

The novel joining technique is suitable for a wide range of applications, e.g. combining LTCC based sensors with injection molded polymer microfluidic systems, integrating transparent polymer windows into non-transparent ceramic systems or joining LTCC systems with cheap polymer connectors to realize a connection to supply units. To exemplify the potentials of the developed joining technique a lab-on-a-chip system was developed. The system is designed to analyze the cellular growth within a microbiological reactor under defined conditions.

References

1. Shen, B., Izquierdo, R., Meunier, M.: Laser fabrication of three-dimensional microstructures, cavities and columns. SPIE **2045**, 91–98 (1994)
2. Lorazo, P., Lewis, L.J., Meunier, M.: Picosecond pulse laser ablation of silicon: a molecular-dynamics study. Appl. Surf. Sci. **168**, 276–279 (2000)
3. Bonseo, J., Baudach, S., Krüger, J., Lenzner, M., Wrobel, J.M., Kautek, W.: Femtosecond pulse laser machining of semiconducting materials. In: Conference Digest. "Conference on Laser and Electro-Optics Europe", Piscataway, NJ, USA (2000)
4. Kaspar, J., Luft, A.: Electron microscopic investigation of structural changes in single crystalline silicon induced by short pulse laser drilling. In: Proceedings of the Micro Materials Conference, p. 539, Hrsg. Michel, B., Winkler, T., Druckhaus Dresden GmbH, Dresden (1997)
5. Lenk, A.: Dissertation Komplexe Erfassung der Energie- und Teilchenströme bei der Laserpulse-Anblation von Aluminium. Department of mathematics and natural sciences, Technical University Dresden, Dresden (1996) (in German)
6. Palik, E.D.: Handbook of Optical Constants of Solids II (Palik, Hrsg.). Academic Press, Inc., New York (1997)
7. Crafer, R.C., Oaklay, P.J.: Processing in Manufacturing, p. 163. Chapman & Hall, London (1993)
8. Klotzbach, U., Hauptmann, J.: Potenzial der Mikromaterialbearbeitung mit UV-Lasern für die Photovoltaik; Laserphotonics. Carl Hanser Verlag GmbH & Co. KG, München (2008) (in German)
9. Hesener, H.: Patent WO 0012/256 "method for processing and for joining, especially, for soldering a component or a component arrangement using electromagnetic radiation" (1999)
10. Patent, V.: Franke WO2008025351: "method for producing a bioreactor or lab-on-a-chip system and bioreactors or lab-on-a-chip systems produced therewith"
11. Franke, V., König, A., Klotzbach, U.: Fest gefügt über Materialgrenzen hinweg Mikroproduktion 4/2007. Carl Hanser Verlag GmbH & Co. KG, München (2007)
12. Klotzbach, U., Franke, V., Sonntag, F., Morgenthal, L., Beyer, E.: Requirements and potentialities for bioreactors with LTCC and polymer. Photonics West, San Jose, CA, USA (2007)

Springer
http://www.springer.com/978-3-642-17781-1

Fabrication and Characterization in the Micro-Nano Range
New Trends for Two and Three Dimensional Structures
Lasagni, F.A.; Lasagni, A.F. (Eds.)
2011, X, 222 p., Hardcover
ISBN: 978-3-642-17781-1